International Journal of Engineering Research & Technology (IJERT)
ISSN: 2278-0181
Vol. 3 Issue 9, September- 2014

Physico-Mechanical and Chemical Properties of Composite Cement Containing High Percentages of Mechanically Activated Egyptian Slag

B. A. Sabrah[1],
[1]Prof. Dr., Chemistry Department,
Faculty of Science, Fayoum University,
Fayoum, Egypt

S. Abd El-Aleem[2]
[2]Ass. Prof. Dr., Chemistry Department,
Faculty of Science, Fayoum University,
Fayoum, Egypt

H. Gouda[3]
[3]Ass. Lecturer, Chemistry Dep.,
Faculty of Science, Fayoum University,
Fayoum, Egypt

***ABSTRACT*- This work aims to study the effect of partial substitution of sulphate resisting cement (SRC) by mechanically activated Egyptian slag on the physico-mechanical and chemical properties of the hardened SRC-GGBFS composite cement pastes and mortars. The SRC was substituted by GBFS up to 75 mass, %. The dry mixes were homogenized in a ball mill to attain complete homogeneity and hydrated with the required water of standard consistency. The degree of hydration of cement pastes was measured by the determination of combined water and free Portlandite contents as well as the pH values. At different mix compositions and curing times, the physico-mechanical properties, i.e., the water of consistency, initial and final setting times, compressive strength and the bulk density were measured. The hydration products of some selected composite cement pastes were investigated using IR, XRD and DSC techniques. It can be concluded that, the substitution of 45-55 mass, % of SRC with GBFS gives composite cement with a reasonable physico-mechanical and chemical characteristics in comparison with those of SRC up to 90 days of hydration.**

Keywords- Hydration characteristics, GGBFS, SRC, composite cements,mechanical properties

I. INTRODUCTION:-

Concrete is one of the critical materials that form the basis of our modern society. Nowadays, more and more consideration is being given to the energy costs and the pollutions of different materials. In this regard, concrete comes out a head of most other materials. The major energy costs and pollution of concrete are in cement. Production of cement accounts for about 5% of the global total CO_2 emissions **[1-3]**. Reduction of energy usage can be taken place even by design methods **[4, 5]** or using supplementary cementitious materials (SCMs) (e.g., granulated blast furnace slag (GBFS), fly ash (FA), and silica fume) in Portland cement concrete, either as amineral admixture or a component of blended cement **[6-8]**. SCMs are actually cheaper and more ‘‘sustainable’’ than cement. When they are used as a partial replacement of cement, suited additions can improve the performance of materials through modifications in physico-chemical properties, as well as the hydration characteristics and microstructure **[9-12]**.Much attention has been paid to using blast furnace slag (BFS) as a potential SCM or aggregate for concrete in order to maximize the economic efficiency and environmental benefits **[13-15]**. The use of BFS as cementitious component requires only grinding; it will save substantial amounts of energy compared with the production of Portland cement, because the grinding process of slag for cement replacement requires only about 25% of the energy needed to Portland cement manufacture **[7]**.BFS is a by-product generated from the manufacture of pig iron. It forms when the slagging agents (e.g., iron ore, coke ash and limestone) are added to the iron ore to remove the contaminated impurities. In the process of reducing iron ore to iron metal, a molten slag forms as nonmetallic liquid (consisting primarily of silicates and aluminosilicates of calcium and other elements) that floats on the top of the molten iron **[16]**. The molten slag is then separated from the liquid metal and cooled by different methods. When the slag is allowed to cool slowly in the air, it solidifies into crystalline material known as air-cooled slag (ACS). But, when it is rapidly and sufficiently cooled by water, it solidifies into granulated form, which known as water-cooled slag (WCS) or granulated blast furnace slag

(GBFS).The chemical composition of slag can vary over a wide range depending on the nature of the ore, the composition of the limestone flux, coke consumption and the type of iron being made. The main constituents of slag include: CaO, SiO_2 and Al_2O_3. In addition, it contains small amount of MgO, FeO and sulphides as CaS, MnO and Fe, which are the most common components in commercial silicate glasses **[17-19]**.GBFS is widely used around the world as SCM, due to its vitreous structure. It shows both cementitious behavior and pozzolanic characteristics in presence of the proper activator **[20, 21]**. GBFS reacts with water at slow rate, due to its glassy structure. Since highly alkaline medium is required to disintegrate the silicate-aluminate network of slag glass. Portlandite (CH) is one of the main hydration products of cement, and it is normally used to provide this alkalinity during the hydration of cement-slag binder **[22-27]**.In previous works **[28-30]**, it was reported that, the reactivity of slag cements depends mainly on its origin, chemical composition and processing (glass content, structure, cooling rate... etc). The reactivity of blended slag-cement pastes with 30-50 mass, % of slag and hydrated at 10-50^{o}C for 6 months was studied **[31]**. The results indicated that, when slag content was increased, its reactivity was reduced. A good indicator of the progress of slag hydration in blended cements is the increase of its pozzolanic reaction rate with free $Ca(OH)_2$. BFS-cement has been often used for civil engineering structures, but it has rarely been used for reinforced concrete buildings because of slow strength development**,** especially at early ages of hydration **[32, 33]**. Hill and Sharp **[34]** studied the hydration products of OPC-GBFS-PFA composites containing higher replacement levels of cement by GBFS (over 60 mass, %) compared with those of OPC. The hydration products were examined by XRD and SEM. The results showed that, $Ca(OH)_2$ was totally consumed within 6 months, indicating the excellent pozzolanic behavior of slag at such high replacement levels.The effect of superfine slag powder on cement propertieswas studied **[35]**. Different blended cements containing 20 up to 80 mass, % of slag were prepared. The heat of hydration, strength and microstructure of hydrated cements were investigated. The results indicated that, the strength of blended cements was lower than that of pure Portland cement. The formation of ettringite, which is mainly responsible for early strength, is influenced by the slag reactivity and sulfate content. At later hydration ages, C-S-H with a low C/S ratio was the dominant hydrate.Khatib et al **[36]** studied some engineering properties of concrete incorporating slag and metakaoline. They concluded that, the partial replacement of Portland cement by GGBFS up to 80 mass% decreases the compressive strength of concrete during the first 28 days, while the later age strength increased with the slag replacement up to 60 mass%**.**

Objective of the research-This work aims to evaluate the physico-mechanical and chemical characteristics of slag rich cements prepared from substitution of different percentages of SRC by GGBFS up to 75 mass%.

II. MATERIALS

The materials used in this study were sulfate resisting cement (SRC) provided from Alexandria Cement Company and granulated blast-furnace slag (GBFS) supplied from Iron and Steel Company, Helwan, Egypt. The chemical analyses of starting materials were given in Table 1. The Blaine surface area of SRC was 3000 ± 50 cm^2/g. The used slag was ground in a laboratory ball mill to the surface area 4000 ± 50 cm^2/g.

III. METHODS AND EXPERIMENTS

A. Preparation of cement specimens

The materials used were dried in an electric drier at 110^{o}C for 24 h to remove the moisture. The crystal structure of the granulated was identified, by means of XRD technique (Fig.1). It shows a hump between 30 and 40^o indicating the presence of amorphous glassy phases. The chemical oxide analyses of SRC and GGBFS in mass, % are listed in Table 1. The mix compositions were prepared as shown in Table 2. The ingredients of each mix were blended in a porcelain ball mill for 1 h using a mechanical roller mill to ensure complete homogeneity, and then the hydration was conducted on cement pastes. The water of consistency and setting times for each mix were determined according to ASTM specification **[37].**The mortars were prepared by mixing 1 part of cement and 2.75 parts of standard sand proportions by weighing with water content sufficient to obtain a flow of 110 ± 5 with 25 drops of the flowing table **[38, 39]**. The freshly prepared mortars were moulded into 50×50×50mm cubic moulds. The specimens were cured for 24 h in 100% RH at 25 ± 2^{0}C, then demoulded and cured under water until the time of testing (3, 7, 28 and 90 days).

B. Stopping of hydration

The hydration of cement pastes were stopped by pulverizing 10g of representative sample in a beaker containing methanol-acetone mixture (1:1), then mechanically stirred for 1h. The mixture was filtered through a gouch crucible, G4 and washed several times with the stopping solution then with ether. The solid was dried at 70^{0}C for 1h complete evaporation of alcohol then collected in polyethylene bags; sealed and stored in desiccators for analysis **[40, 41]**.

C. Determination of chemically combined water and free lime contents

Chemically combined water contents(Wn,%)of each mix was determined as the percent of ignition loss of the dried samples (on the ignited weight basis) **[42,43]**. The free lime content (FL, %) was determined by an ammonium acetate method **[44, 45]**.

D. Determination ofbulk densityand compressive strength

The bulk density (BD) was carried out on cement pastes. Samples were suspended weighed in water and in

air (saturated surface dry). Each measurement was conducted on at least three similar cubes of the same mix composition and curing time. Then, the density was calculated as described elsewhere **[46]**. Compressive strength was determined according to ASTM (C-150) **[47]**; a set of three cubes was tested on a hydraulic universal testing machine (ADR) of 2000 KN capacity.

E. XRD, DSC and IR techniques

To verify the mechanism predicted by the chemical and mechanical tests, some selected hydration products were investigated using XRD, DSC and IR techniques. The powder method of X-ray diffraction was adopted in the present study. For this, a Philips diffractometer PW 1730 with X-ray source of Cu kα radiation (λ=1.5418Å) was used. The scan step size was 2θ, the collection time 1s, and in the range of 2θ from 5 to 65^o. The X-ray tube voltage and current were fixed at 40 KV and 40 mA respectively **[48]**. Differential scanning calorimetery was carried out using DSC-50 thermal analyzer at a heating rate of 10^{o}C/min., in the temperature range up to 300^{o}C. The samples chamber was purged with nitrogen at a flow rate of 30^{o}C /min. For IR spectroscopic investigation, the samples were prepared using alkali halide KBr disks using Gensis FT-IR spectrometer in the range 400-4000cm^{-1} after 256 scans at 2cm^{-1} resolution **[49]**.

IV. RESULTS AND DISCUSSIONS

A .Water of consistency and setting times

The water of consistency (W/C, %) as well as initial and final setting times of the investigated cement pastes are graphically represented in Fig.2. It is clear that, the substitution of 45 mass, % SRC with GGBFS is accompanied by a sharp decrease of water of consistency. As the slag content increases up to 75 mass, % the water of consistency is slightly decreased. Also, the setting times are elongated with slag content. This is attributed to the lower hydraulic properties of slag in comparison with SRC as a result of acidic oxide film formation on the outer layer of slag **[50]**.

B. Bulk density

The variation of bulk density of the hydrated cement mixes are plotted as a function of curing time up to 90 days in Fig.3. The results show that, the bulk density of all cement mixes increases with curing time. As the hydration proceeds, more hydrated products are precipitated in the water filled pores, leading to the formation of compact structure. At a given curing time, the bulk density for SRC is higher than that of blended slag cements, because the hydration products of blended slag cements contain CSH with low C/S ratio and low density in comparison with that formed from the hydration of cement clinker phases **[51].**

C. Compressive Strength

The compressive strength of cement mortars cured in tap water up to 90 days is plotted in Fig.4. Generally, the compressive strength for all cement mortars increases with curing time, due to the continuous hydration and formation of hydrated silicates (CSH), aluminates (CAH) and aluminosilicates (CASH). Also, the compressive strength of blended slag cement mortars increases with curing time. This is attributed to the pozzolanic reaction of the slag portion with the liberated lime (CH) from the hydration of SRC clinker phases **[36]**, leading to the formation and accumulation of additional CSH, CAH and CASH, which responsible for strength properties. The results also indicate that, the strength values decrease with the GGBFS, %, due to the slower hydration rate of slag in comparison with SRC at early ages of hydration. But, at later ages, the pozzolanic activity of slag enhances, therefore the compressive strength of blended slag cements may reach that of SRC. It can be reported that, the substitution of 45 to 55 mass, % of SRC with GGBFS shows nearly the same compressive strength as SRC itself at 90 days of hydration.

D. Chemically combined water contents

The combined water contents (Wn, %) of the hydrated SRC and blended slag cements are graphically shown in Fig.5. It can be seen that, Wn% increases with curing time for all hydrated cement pastes, due to the continuous hydration of cement clinker phases in addition to the activation of the slag portion in the presence of $Ca(OH)_2$. The blended slag cements give lower values of combined water than those of SRC, due to the higher hydraulicity of SRC in comparison with GGBFS. Wn% decreases with slag content, due to the fact that, the hydration of blended slag cements produces hydrated silicates and aluminosilicates with lower water contents than those formed from the hydration of SRC, besides the consumption of $Ca(OH)_2$ by pozzolanic reaction with slag, leading to the decrease of Wn%. It was reported that, the combined water contents of pozzolanic cements are lower and their porosities are higher than the comparable Portland cement **[52]**, because the replacement of CH by CSH or CASH causes relatively little change in the H_2O/Ca ratio.

E. Free lime

The free lime values (FL, %) of the hydrated cement mixes are represented graphically as a function of curing time and slag content in Fig.6. The results illustrate that, FL% of SRC pastes increases linearly with curing time up to 90 days, due to the continuous hydration of cement clinker, liberating free lime. On the other hand, FL% of blended slag cements decreases with curing time and slag percentage. The decrease of free $Ca(OH)_2$ with hydration time is due to two processes work in opposite directions, the first is the continuous hydration of cement clinker, which produces lime, and the second is the increase of pozzolanic activity of slag with curing time, leading to consumption of some portlandite, but the rate of lime consumption exceeds that of lime production with. Also, free lime content decreases with GBFS%. This is

attributed to the decrease of SRC content, which liberates free lime as well as the increase of slag portion, which consumes the liberated Portlandite during the hydration of clinker phases **[53, 54]**.

F. pH-values

The variation of pH values of the investigated cement pastes with curing time up to 90 days is plotted in Fig.7. It is clear that, the pH-value increases with curing time for SRC mixes, due to the continuous hydration of cement clinker phases and liberating Ca^{2+}, which increases the pH value. The pH values of blended slag cements decrease with curing time as well as GBFS%, due to the continuous consumption of CH with slag content. As the slag content increases, the pH value decreases due to the decrease of SRC% and consequently the liberated lime, which is the main factor affecting pH value. The results of pH are in a good agreement with those of free lime.

G. IR Spectroscopy

Fig.8 represents FT-IR spectra of anhydrous GBFS. It contains two main bands at 492 and 988 cm^{-1} as well as less intense two bands at 717 and 1422 cm^{-1}. The appeared bands at 988 and 492 cm^{-1} refer to the presence of orthosilicate units $[Si_2O_7]^{6-}$ with partial substitution of Si^{4+} by Al^{3+} in tetrahedral positions. These units are built of two silico-oxygen (or silico/and alumino-oxygen) tetrahedral, connected with oxygen bridge. The two bands at 988 and 492 cm^{-1} represent the vibrations of $[SiO_4]^{4-}$ and $[AlO_4]^{5-}$ tetrahedral**.** The first refers to Si-(Al)-O anti symmetric stretching vibrations; the second should be assigned to bending vibration of O–Si–O bonds **[55].** The appearance of the most intense bands at relatively low wave numbers proves that, the silicate phases occurring in GBFS containing orthosilicate units $[Si_2O_7]^{6-}$. The existence of the weak band at 716 cm^{-1}, assigns to the symmetric stretching vibrations of the Si–O–Si(Al) bridges, and further confirms the presence of these units. It is also connected with vibrations of Si-O-Al bridges, formed by linkage of $[SiO_4]^{4-}$ and $[AlO_4]^{5-}$ tetrahedral **[56].** Moreover, it is impossible to exclude the association of this band with Al–O vibrations, appearing in aluminosilicates octahedral. High content of aluminum also causes the location of the 988 cm^{-1} band at such low wave number. Aluminum atoms in tetrahedral coordination influence a shift of the most intense band to lower wave numbers, in relation to 1100 cm^{-1} position characteristic for pure silica spectra in non-hydrated form **[57].** Low intensity band at 1422 cm^{-1} originates from a low number of carbonate groups $[CO_3]^{2-}$. Absorption bands at 1642 and 3441 cm^{-1} are due to the bending vibration of H- OH and stretching of O-H group as moisture content in slag. High full width at half maximum (FWHM), especially noticeable in the case of the most intense band at 988 cm^{-1} proves the significant content of glassy phase in slag structure. It is well known that, the phases of non-ordered structure cause the increase in the band width due to the existence of significant fluctuations of geometric parameters. The shape of the described spectra is typical of glassy aluminosilicates belonging to the groups of gehlenites and melinites**[58].**

FTIR spectra of M_0, M_2 and M_4 cured for 28 days are shown in Fig.9. A small peak appears at 3637-3641 cm^{-1} due to the –OH band from $Ca(OH)_2$, this band is useful for diagnosis the hydration process**[59],** its intensity decreases with slag content, due to pozzolanic reaction. The broad stretching band centered at about 3400 cm^{-1} as well as bending at1640-1650 cm^{-1} is attributed to vibration water in the hydration products such as CSH, CAH and ASH. The appeared band around 950-980 cm^{-1} may be assigned to the formation of CSH**,** its intensity decreases with slag content. The band at 1475 cm^{-1} is attributed to stretching vibration of C—O bond in CO_3^{2-}, which results from the carbonation of hydration products. The intensity of that band decreases with slag content up to 55 mass%, then increases up to 70 mass% GBFS .This may be due to the higher porosity of slag rich cement pastes than that of SRC. The bands at 671-717 and 450-492 cm^{-1} are related to symmetric stretching vibrations of the Si—O—Si (Al) bridges and bending vibrations of O—Si—O bonds respectively. The appeared band at 970 cm^{-1} may be due to the alumina content and refers to Si(Al)—O anti-symmetric stretching vibration. Its intensity increases with GBFS content **[60]**.This can be illustrated from the chemical analysis of starting materials where GBFS contains higher alumina content than SRC.

The effect of curing time of M_0 can be seen from IR spectra at 3, 28 and 90 days in Fig.10. The observed peak at 3637-3641 cm^{-1} is assigned to the –OH group of calcium hydroxide. The intensity of that peak increases with curing time up to 90 days, due to the progress of hydration reaction of cement clinker phases liberating free lime.The appeared band at the range 950-980 cm^{-1} may be assigned to the formation of CSH. Also, its intensity increases with curing time, due to the enhancement of the hydration reaction of cement phases, leading to the formation of additional amounts of CSH. The broad band centered at about 3400 cm^{-1} and the band observed at 1640-1650cm^{-1} are assigned to stretching and bending vibration of combined water in the hydration products. Their intensities increase with curing time, due to the continuous hydration of clinker phases, leading to the formation of excessive amounts of hydrated compounds with high water contents. The band at 1475 cm^{-1} is attributed to C—O bond stretching of CO_3^{2-}, which results from the carbonation of the hydration products as well as the residual portlandite, $Ca(OH)_2$. The intensity of that band increases with curing time due to the increase of F.L%.

H. Thermal analysis

Fig. 11 illustrates the DSC thermograms of M_0, M_2 and M_4 hydrated up to 28 days. The results show endothermic effects at 250^{0}C, 477-480^{0}C as well as a broad peak in the range 575-700^{0}C. The endothermic peaks located at 250^{0}C are related to the decomposition of CSH, calcium sulfoaluminate and chloroaluminate hydrates as well as hydrogarnet. The endothermic peaks located at 477-480^{0}C is related to the dehydration of portlandite or free $Ca(OH)_2$, whereas the broad endotherm at 600-700^{0}C is due to the decomposition of $CaCO_3$. Also, the area of endothermic peak decreases with the GBFS% (from 0.0 up

to 75.0 wt., %). The heat enthalpy decreases in the same direction. The results of DSC analysis are in a good harmony with those of chemical analysis.

DSC thermograms of M_0 hydrated at 3, 28 and 90 days are represented in Fig.12. It is clear that, the intensity of portlandite peak increases with curing time, due to the continuous hydration of cement phases, liberating free lime. Therefore, the quantity of $Ca(OH)_2$ increases from 3 days up to 90 days. This is also seen from the heat enthalpy. The endothermic peaks of CSH and calcium sulfoaluminate, chloroaluminate hydrates as well as hydrogarnet, increase, due to the formation of more amounts of these hydrates with curing time.

Fig.13 represents DSC thermograms of M_2 at different curing time (3, 28 and 90 days). It is clear that, the intensity of portlandite peak decreases with curing time, due to its consumption during the pozzolanic reaction with GBFS. Therefore, the quantity of $Ca(OH)_2$ decreases from 3 up to 90 days. In contrast the intensities of hydrated calcium silicate, calcium sulfoaluminate and hydrogarnet, increase with the time. The observed endothermic peak at 650^0C is assigned to the decomposition of $CaCO_3$.

I.Interpretation of XRD results

XRD patterns of SRC as well as blended cement pastes with 55 and 75% GBFS and hydrated for 28 days are shown in Fig.14. XRD patterns show the formation of hydrated phases portlandite and CSH due to the hydration of C_3S and β-C_2S present in cement pastes as well as the presence of anhydrous dicalcium and tricalcium silicate. Cement paste with 55 mass% GBFS represents the formation of $C_{1.5}S_{3.5}$.xH in addition to the liberated lime with anhydrous C_2S. As the slag content increases up to 75 mass%, the patterns illustrate the presence of free $Ca(OH)_2$ with hydrated CSH and anhydrous β-C_2S. The addition of GBFS increases the S/C ratio.

XRD patterns of M_2 pastes hydrated in tap water up to 90 days are shown in Fig.15. It is clear that, the hydration products are mainly CSH with various C/S ratios, portlandite and anhydrous β-C_2S. Cement paste at 3 days shows the C/S ratio $C_{1.5}S_{2.0}$.xH. As the hydration proceeds up to 28 days, the CSH molar ratio changes to $C_{1.5}S_{3.5}$.xH. This is mainly due to the reaction of silica from GBFS with portlandite. The hydrated sample at 90 days shows the same molar ratio, due to the continuous consumption of $Ca(OH)_2$ with curing time.

V. SUMMARY AND CONCLUSIONS

By means of an experimental program concerning the hydration kinetics of blended slag rich cements as well as that of SRC were followed by different tests such as, determination of free lime, combined water, and pH value as well as the bulk density and compressive strength of the hydrated mixes up to 90 days. Also, the hydration products of some selected mixes were analyzed using XRD, DSC and FTIR techniques. From the results in hand, it can be concluded that:Substitution of SRC by GGBFS reduces the mixing water, elongates the initial and final setting times and decreases the combined water contents.As the slag% increases, the free lime and pH values decrease. It seems to be due to the consumption of some Ca(OH)2 with GBFS in pozzolanic reaction. The values of bulk density of SRC and slag rich cement pastes increase with curing time, due to the continuous hydration and accumulation of hydration products in some of the open pores, originally filled with water, resulting in the formation of homogeneous and dense structure. The dp values of SRC mixes are higher than those of blended slag cements. As the slag content increases, the bulk density decreases. At early ages of hydration, the compressive strength decreases with the GBFS%, due to the slower hydration rate of slag in comparison with SRC. At later ages, the pozzolanic activity of slag enhances, therefore the compressive strength of blended slag cements may reach or exceed that of SRC. The results of XRD, DSC and FTIR analyses are in a good harmony with each other and with those of the chemical and physico-mechinal properties.The substitution of 45-55 mass% of SRC with GBFS gives a reasonable hydration characteristics and improved mechanical properties nearly to those of SRC up to 90 days of hydration.

VI. REFERENCES

[1] W. Ernst, P.Lynn, and M. Nathan, "Carbon dioxide emissions from the global cement industry" Annu. Rev. Energ. Environ., 26; (2001), pp. 303-329.

[2] M. Heikal, M.Y. Nassar, G. El-Sayed, S.M. Ibrahima,"Physico-chemical, mechanical, microstructure and durability characteristics of alkali activated Egyptian slag", Constr. Build.Mater., 69 (30) ; (2014), pp. 60-72.

[3] K. Gu, F. Jin, A. Al-Tabbaa, B. Shi, and J. Liu, "Mechanical and hydration properties of ground granulated blast furnace slag pastes activated with MgO–CaO mixtures", Constr. Build. Mater., 6 (30); (2014), pp. 101-108.

[4] L. Gustavsson, A. Joelsson, "Life cycle primary energy analysis of residential buildings", Energy and Buildings, 42 (2); (2010), pp. 210–220.

[5] G.A. Blengini, T. Di Carlo, "The changing role of life cycle phases, subsystems and materials in the LCA of low energy buildings", Energy and Buildings, 42 (6); (2010), pp. 869–880.

[6] C. Becchio, S.P. Corgnati, A. Kindinis, S. Pagliolico, "Improving environmental sustainability of concrete products: investigation on MWC thermal and mechanical properties", Energy and Buildings, 41 (11); (2009), pp. 1127–1134.

[7] C. Shi, J. Qian, "High performance cementing materials from industrial slags: a review", Resources, Conservation and Recycling 29; (2000), pp. 195–207.

[8] R. Demirbo˘ga, "Influence of mineral admixtures on thermal conductivity and compressive strength of mortar", Energy and Buildings, 35 (2); (2003), pp. 189–192.

[9] A. Bentur, "Cementitious materials-Mine millennia and a new century: Past, present, and future", J. Mater. Civ. Eng., 14; (2002), pp. 1–22.

[10] P. K. Mehta "Greening of the concrete industry for sustainable development", Concr. Int., 24; (2002), pp. 23–28.

[11] W. Qiang, Z. Bo and Y. Yu, "The influence of steel slag with high Al_2O_3 content on the initial hydration of cement", Sci. China Tech. Sci., 56 (12) ; (2013), pp. 3123–3128.

[12] K. Hanna, G. Morcous and M. K. Tadros, "Effect of Supplementary Cementitious Materials on the Performance of Concrete Pavement", J. Mater. Civ. Eng. 26; (2014), pp. 789-793.

[13] V. Kocaba, E. Gallucci and K. L. Scrivener, "Methods for determination of degree of reaction of slag in blended cement pastes", Cem.Concr.Res., 42; (2012), pp. 511–525.

[14] H .Motz and J.Geiseler, "Products of steel slags—an opportunity to save natural resources", Waste Manage, 21(3); (2001), pp. 285–93.
[15] C. Li, H. Sun and L.Li, "A review: The comparisonbetween alkali-activated slag (Si+ Ca) and metakaoline (Si+ Al)cements", Cem. Concr. Res., 40; (2010), pp. 1341-1349.
[16] R. Siddique, "Waste materials and by-products in concrete", Berlin (Heidelberg): Springer-Verlag; (2008).
[17] S. Kumar, R. Kumar, A. Bandopadhyay, T. C. Alex, B. Ravi Kumar, S.K. Das and Mehrotra S.P., "Mechanical activation of granulated blast furnacslag and its effect on the properties and structure of Portland slagcement", Cem. Concr.Compos., 30; (2008), pp. 679-685.
[18] C.J. Shi and J.S. Qian, "High performance cementing materials from industrial slags – a review ".Resour. Conserv.Recy., 29 (3); (2000), pp. 195–207.
[19] X.Q.Wu, H. Zhu, X.K. Hou and H. Li, "Study on steel slag and fly ash composite Portland cement", Cem. Concr. Res., 29 (7); (1999), pp. 1103–6.
[20] B. Kolani, L. B. Lacarrière, A. Sellier, G. Escadeillas, L. Boutillon and Linger L., "Hydration of slag-blended cements", Cem. Concr.Compos., (34); (2012), pp. 1009-1018.
[21] S. Abd El-Aleem, "Hydration characteristics of granulated slag with fired by-pass cement dust", Sil. Ind; 69(3-4); (2004), pp. 46-52.
[22] S.C. Pal, A. Mukherjee, S.R. Pathak, "Investigation of hydraulic activity of ground granulated blast furnace slag in concrete", Cem. Concr. Res 33; (2003), pp. 1481–6.
[23] S.J. Song and M.J. Hamlin, "Pore solution chemistry of alkali-activated ground granulated blast-furnace slag", Cem.Concr. Res., 29; (1999), pp. 159-70.
[24] S. Kumar, R. Kumar, A. Bandopadhyay and T.C. Alex, "Mechanical activation of granulated blast furnace slag and its effect on the properties and structure of Portland slag cement", Cem. Concr.Compos. 30; (2008), pp. 679-85.
[25] Q. Wang, P. Yan and G. Mi, "Effect of blended steel slag–GBFS mineral admixture on hydration and strength of cement", Constr.Build. Mater, 35; (2012), pp. 8-14.
[26] T. Saeki and P.J.M. Monteiro, "A model to predict the amount of calcium hydroxide in concrete containing mineral admixtures", Cem.Concr. Res., 35; (2005), pp. 1914-21.
[27] I. Pane and W. Hansen, " Investigation of blended cement hydration by isothermal calorimetry and thermal analysis", Cem. Concr. Res., 35; (2005), pp. 1155–64.
[28] A. Bougara, C. Lynsdale and Milestone N.B., " Reactivity and performance of blast furnace slags of differing origin", Cem. Concr.Comos., 32; (2010), pp. 319–24.
[29] X. Zhu, H. B. Hou, X. Q. "Huang, et al. Enhance hydration properties of Steel slag using grinding aids by mechano-chemical effect", Constr. Build. Mater., 29; (2012),pp.476–481.
[30]Q. Wang, P. Y. Yan, J. W. Feng, "A discussion on improving hydration activity of steel slag by altering its mineral compositions". J Hazard Mater, 186; (2011), pp. 1070–1075.
[31] J.I. Escalante, L.Y. Gomez, K.K. Johal, G. Mendoza, H. Mancha and J. Mendez, "Reactivity of blast-furnace slag in Portland cement blends hydrated underdifferent conditions", Cem. Concr. Res., 31; (2001), pp. 1403-9.
[32] S. Miyazawa, T. Yokomuro, E. Sakai, Atsushi Yatagai, NobukazuNito, Kiyoshi Koibuchi "Properties of concrete using high C_3S cement with ground granulated blast-furnace slag" , Construction and Building Materials 61; (2014), pp. 90–96.
[33] P.K. Mehta and P.J.M. Monteiro, Concreto. Estrutura, propriedades e materiais, third ed. São Paulo: IBRACON; 2008. 12- Q. Niu, N. Feng, J. Yang and X. Zheng, "Effect of superfine slag powder on cement properties", Cem. Concr.Res., 32(4); (2002), p. 615.
[34] J. Hill and J.H. Sharp, "The mineralogy and microstructure of threecomposite cements with high replacement levels", Cem. Concr.Comp., 24(2);(2002), p. 191.
[35] Q. Niu, N. Feng, J.Yang and X. Zheng, "Effect of superfine slag powder on cement properties", Cem.Concr.Res., 32(4); (2002), p. 615.
[36] J.M. Khatib and J.J. Hibbert, "Selected engineering properties of concrete incorporating slag and metakaoline", Constr. Build.Mater.,19(6); (2005), pp. 460-72.
[37]ASTM Designation: C191,Standard method for normal consistencyand setting of hydraulic cement, ASTM Annual Book of ASTMStandards,o4.01; (2008).
[38] A. M. Abdelaziz, S. Abd El-Aleem and W. M. Menshawy, "Effect of fine materials in local quarry dusts of limestone and basalt on the properties of Portland cement pastes and mortars", International Journal of Engineering Research & Technology (IJERT), 3 (6); (2014), pp.1038-1056.
[39] M. Heikal, S. Abd El-Aleem, and W.M. Morsi, "Characteristics of blended cements containing nano-silica", HBRC Journal ,9; (2013), pp. 243–255.
[40] M.A. Abd-El.Aziz, S. Abd.El.Aleem, and M. Heikal, "Physico-chemical and mechanical characteristics of pozzolanic cement pastes and mortars hydrated at different curing temperatures", Constr. Build. Mater, 26; (2012), pp. 310–316.
[41]S.Abd. El. Aleem, M. Heikal, W. M.Morsi, "Hydration characteristic, thermal expansion and microstructure of cement containing nano-silica", Constr. and Build.Mater., 59(30) ; (2014), pp. 151-160.
[42] S. Abd El-Aleem, M.A. Abd-El-Aziz,M. Heikal, and H. El Didamony, "Effect of cement kiln dust substitution on chemical and physical properties and compressive strength of Portland and slag cements ", The Arabian Journal for Science and Engineering, 30; (2005), pp. 263-273.
[43] E. A. El-Alfi, A. M. Radwan, and S. Abed El-Aleem,"Effect of limestone fillers and silica fume pozzolana on the characteristics of sulfate resistant cement pastes", Ceramics -Silikáty, 48 (1) ; (2004), pp. 29-33.
[44] S. Abd El-Aleem and A. Ragab, "Physico-mechanical properties and microstructure of blended cements incorporating nano-silica", International Journal of Engineering Research & Technology (IJERT), 3 (7); (2014), pp. 339-358.
[45] H.W.Sufee, "Comprehensive studies of different blended cements and steel corrosion performance in presence of admixture", Ph.D. Thesis, FacultyofScience, Fayoum University, Fayoum,Egypt, (2007).
[46] H. H. Assal, "Some studies on the possibility utilization of calcareous shale/clay deposits in building bricks industry", Ph. D. Thesis, facultyofscience, Zagazig university, Zagazig, Egypt, (1995).
[47] ASTM C109, "Strength test method for compressive strength of hydraulic cement mortars",(2007).
[48] V.S. Ramachandran, Thermal Analysis, in; "Handbook of analyticaltechniques in concrete science and technology", V.S. Ramachandran and J. J. BeaudoinEds., Noyes publications, New Jersey, 2001. ISBN: 0-8155-1473-9.
[49] R.J. Errington, "Advanced Practical Inorganic and Metal 0rganic Chemistry". BalckieAcadamic Professional, AnImpient Chapman&Hall, (1997).
[50] H. El-Didamony, M. Abd-El. Eziz and Abd. S. El.Aleem, "Hydrationand durability of sulfate resisting and slag cement blends in Qaron'sLake water", Cem. Concr. Res., 35; (2005), pp. 1592-1600.
[51] H.F.W. Taylor, Cement Chemistry. 2nd ed. London:Thomas Telford Publishing; (1997).
[52] A. M. Harrison, N. B. Winter and H. F. W. Taylor,Mater. Res. Soc. Sym. Proc.,85; (1987), p. 213.
[53] S. Mindess, F.J. Yonug and D. Darwin, Concrete, 2nd ed., Upper Saddle River: Prentice Hall (2003).
[54] J. X. Li, Q. J. Yu and J. X. Wei, " Structural characteristics and hydration kinetics of modified steel slag", CemConcr Res,41; (2011), pp.324–329.
Composites.34(9); (2012), pp.1009–1018.
[55] M. Griado, A. Fernandez-Jimenez and A. Palomo, "Alkali activationof fly ash: effect of the SiO_2/Na_2O ratio", Part I: FTIR study,MicroporousMesoporous Mater., 106; (2007), pp. 180-191.
[56] K. Ishida, D.M. Jenkins and F. C. Hawthorne, A. M. Mineral, 93; (2008), p. 1112.
[57] J. Zhang, J. L. Provis, D. Feng and J. S .J Deventer Van, "Geopolymersfor immobilization of Cr^{6+}, Cd^{2+} and Pb^{2+}", J Hazard. Mater., 157(2/3); (2008), pp. 587-598.
[58] G. E. De Benedetto, R. Laviano, L. Sabbaini and P.G. Zambonin, "Infrared spectroscopy in the mineralogical characterization of ancient pottery", J. Cult. Heritage, 3(3); (2002), pp. 177-186.

[59] J. Bensted, "Applications of Infrared Spectroscopy to cementhydration", paper delivered at the Construction Materials Groupand Institute of materials meeting on techniques forcharacterization of cement hydration, London Society ofChemicalIndustry, (1994).
[60] A. H. Delgado, R.M. Paroli and J.J. Beaudoin, "Comparison of IR techniques for the characterizationofconstructioncementminerals and hydrated products", Applied Spectroscopy, 50(8); (1996), pp. 970-976.

Table (1):Chemical oxide analyses of SRC and GGBFS (mass, %)

Materials / Oxides	SRC	Slag
SiO_2	19.35	41.79
Al_2O_3	4.19	8.77
Fe_2O_3	5.19	0.57
CaO	62.39	36.64
MgO	2.79	5.43
SO_3	2.18	1.21
K_2O	0.28	0.63
Na_2O	0.62	0.13

Table (2): Mix composition of blended cements in mass, %

Mix No.	SRC	GGBFS
M_0	100	0
M_1	55	45
M_2	45	55
M_3	35	65
M_4	25	75

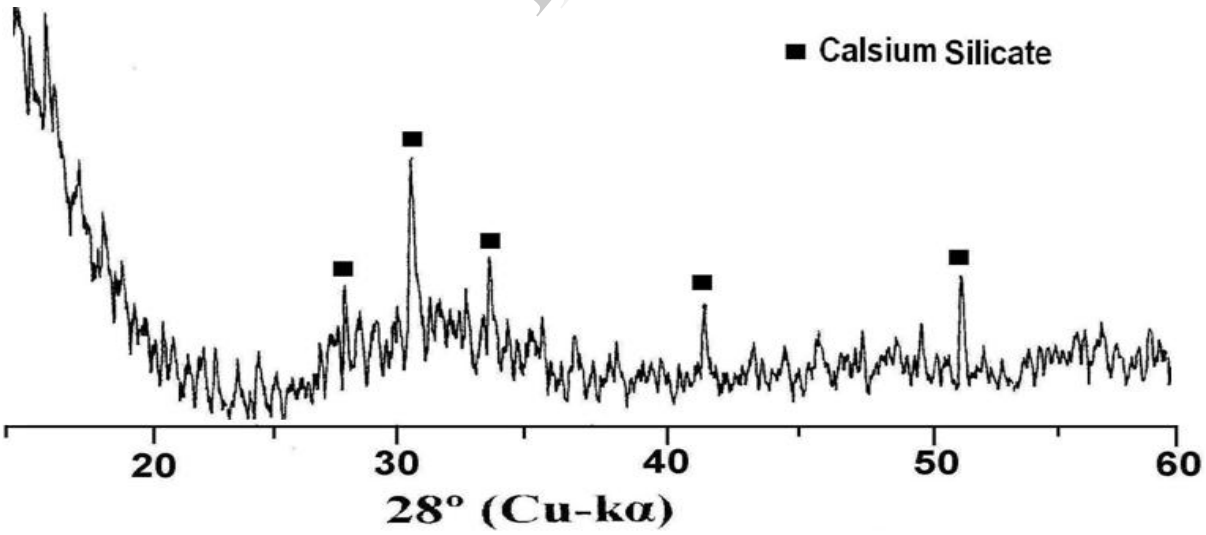

Fig.1. XRD pattern of GGBFS

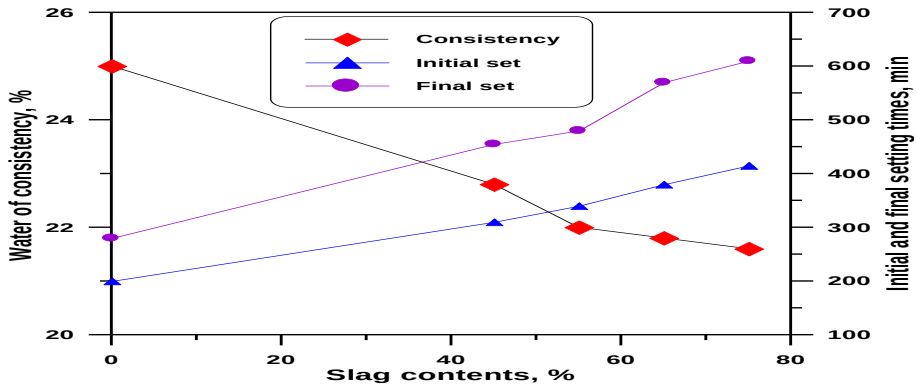

Fig.2. Water of consistency and setting times of the investigatedcement pastes

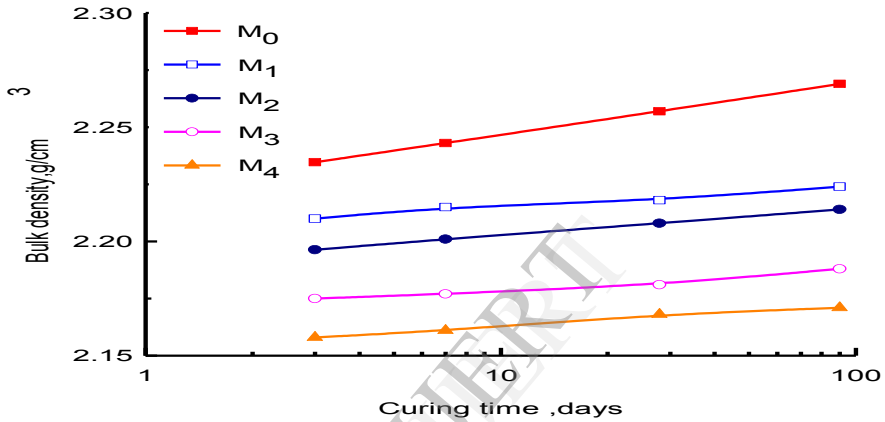

Fig.3. Bulk density of the hardened cement pastes as a function of curing time

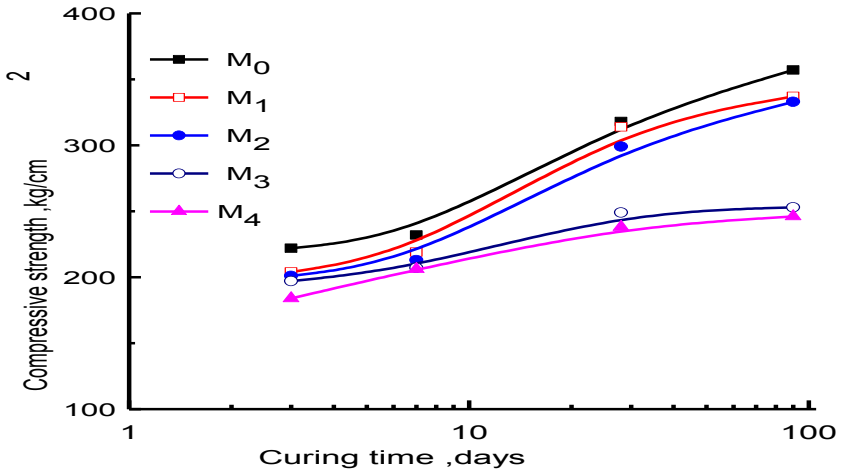

Fig.4.Compressive strength of the hardened cement mortars as a function of curing time

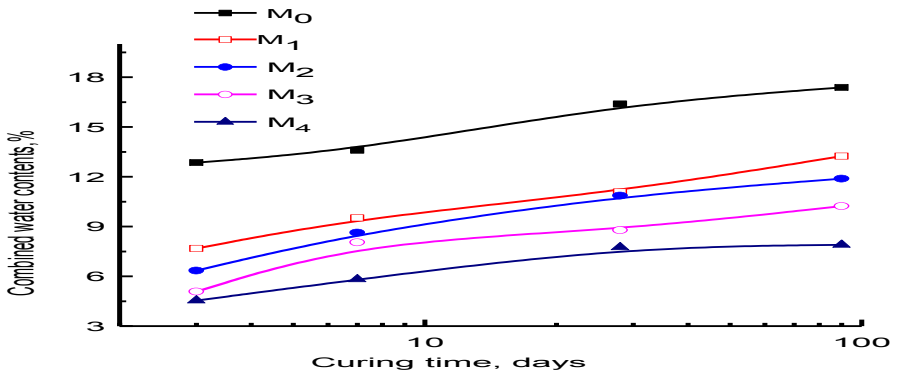

Fig.5. Combined water contents of the hydrated cement pastes as a function of curing time

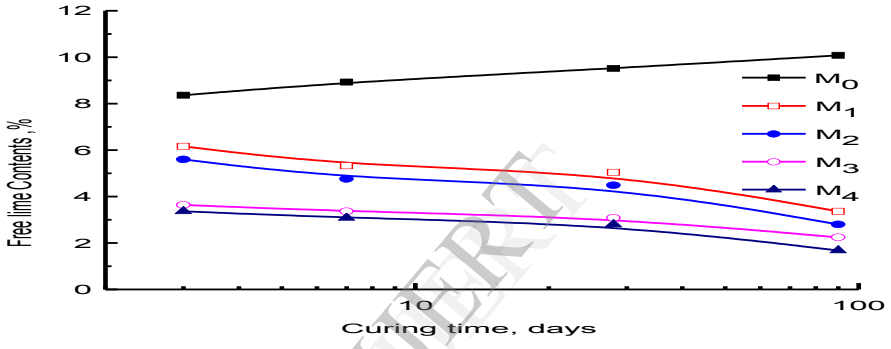

Fig.6. Free lime contents of the hydrated cement mixes as a function of curing time

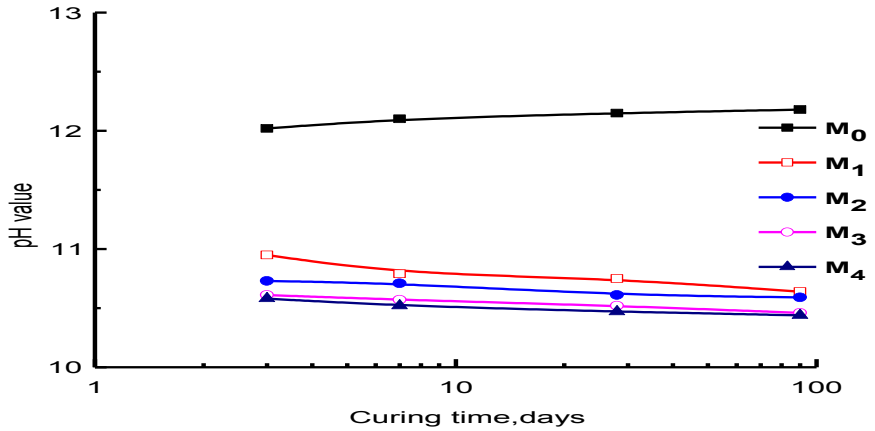

Fig.7. pH values of the hydrated cement pastes as a function of curing time

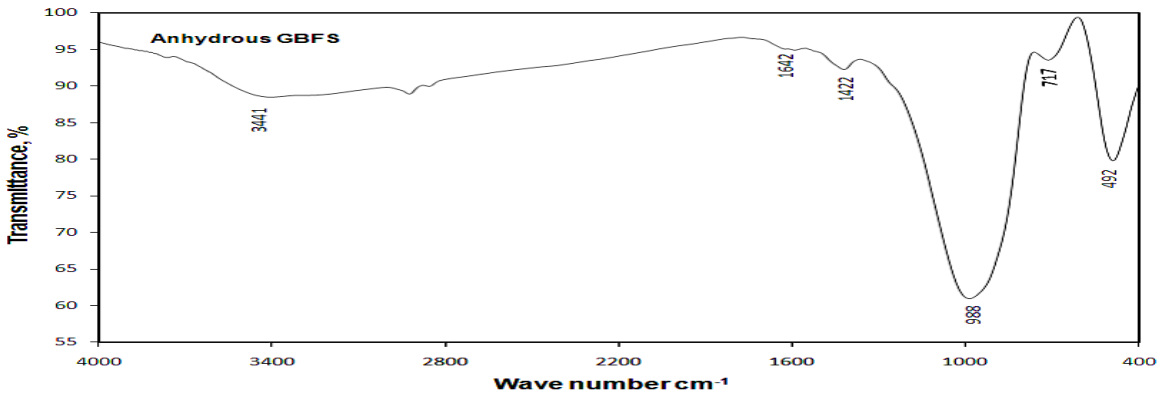

Fig.8. FT-IR spectra of anhydrous GBFS

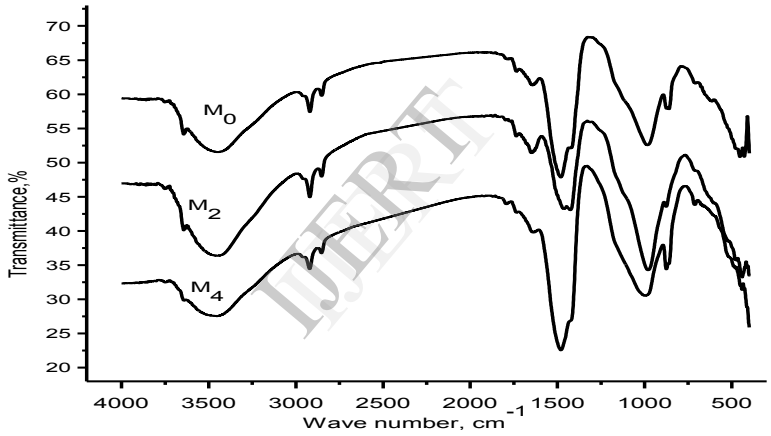

Fig.9.IR-spectral of the hydrated cement pastes at 28 days

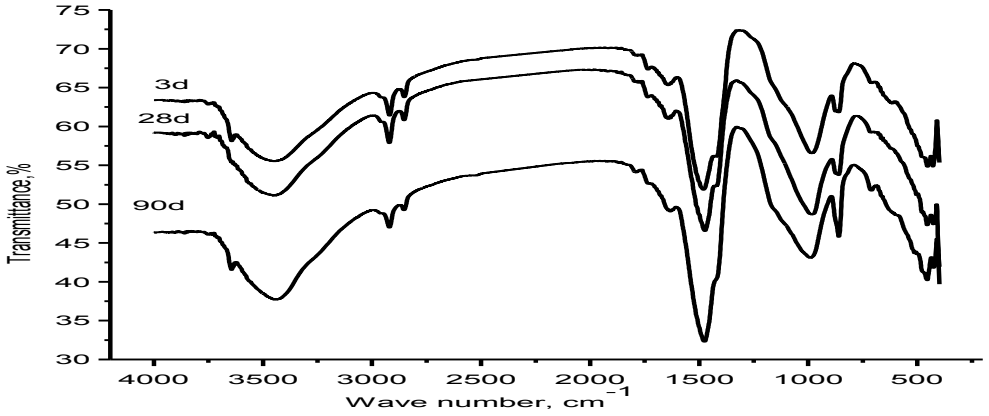

Fig.10. IR-spectral of hydrated pastes of M_O up to 90 days

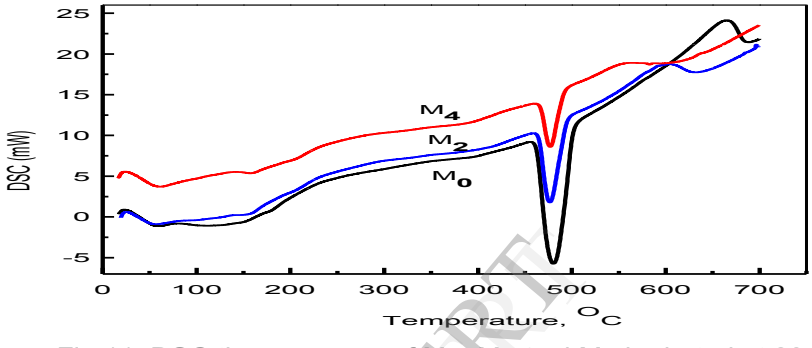

Fig.11. DSC thermograms of M_0, M_2 and M_4 hydrated at 28 days

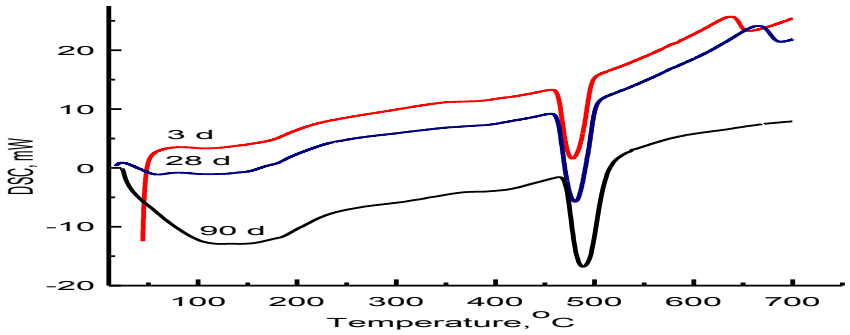

Fig.12. DSC thermogram of M0 hydrated at different curing times up to 90 days

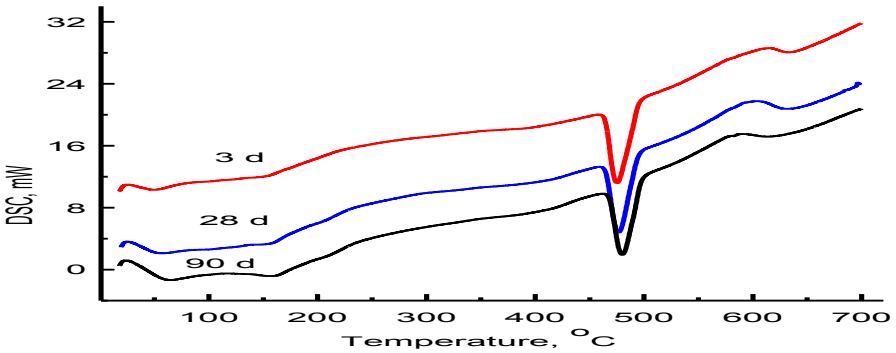

Fig.13. DSC thermograms of M_2 cement pastes at different curing times up to 90 days

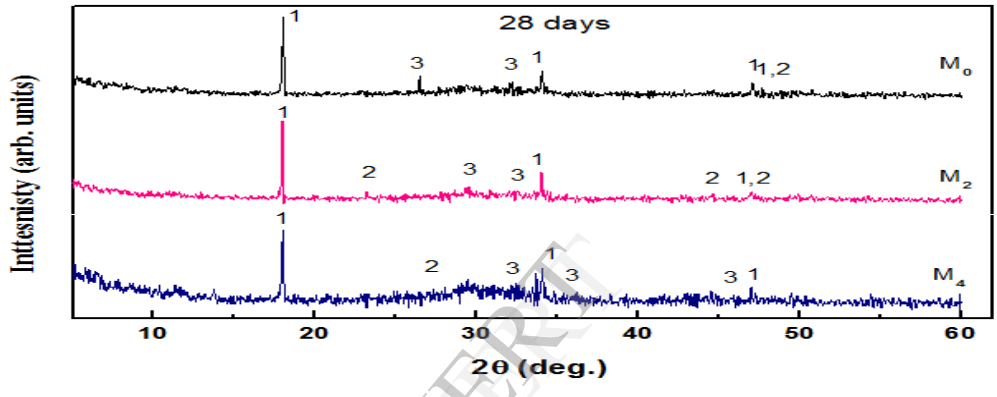

Fig.14.XRD patterns of the hydrated cement pastes at 28 days

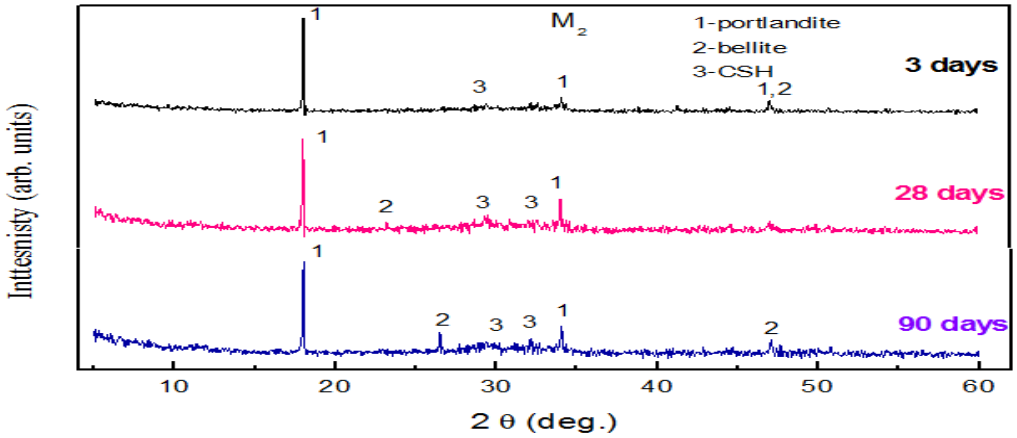

Fig.15.XRD patterns of M_2 pastes hydrated at differentcuring times